

Transmission of vertical soil stress under agricultural tyres: Comparing measurements with simulations



T. Keller^{a,b,*}, M. Berli^c, S. Ruiz^d, M. Lamandé^e, J. Arvidsson^b, P. Schjønning^e, A.P.S. Selvadurai^f

^a Agroscope, Department of Natural Resources & Agriculture, Reckenholzstrasse 191, CH-8046 Zürich, Switzerland

^b Swedish University of Agricultural Sciences, Department of Soil & Environment, Box 7014, SE-75007 Uppsala, Sweden

^c Desert Research Institute, Division of Hydrologic Sciences, 755 E. Flamingo Road, Las Vegas, NV, USA

^d Swiss Federal Institute of Technology, Soil and Terrestrial Environmental Physics, Universitätsstrasse 16, CH-8092 Zürich, Switzerland

^e Aarhus University, Department of Agroecology, Research Centre Foulum, Blichers Allé 20, Box 50, DK-8830 Tjele, Denmark

^f McGill University, Department of Civil Engineering and Applied Mechanics, 817 Sherbrooke Street West, Montréal, QC, H3A 0C3 Canada

ARTICLE INFO

Article history:

Received 31 July 2013

Received in revised form 5 March 2014

Accepted 6 March 2014

Keywords:

Soil stress

Stress transmission

Elasticity theory

Concentration factor

Modelling

ABSTRACT

The transmission of stress induced by agricultural machinery within an agricultural soil is typically modelled on the basis of the theory of stress transmission in elastic media, usually in the semi-empirical form that includes the “concentration factor” (ν). The aim of this paper was to measure and simulate soil stress under defined loads. Stress in the soil profile at 0.3, 0.5 and 0.7 m depth was measured during wheeling at a water content close to field capacity on five soils (13–66% clay). Stress transmission was then simulated with a semi-analytical model, using vertical stress at 0.1 m depth estimated from tyre characteristics as the upper boundary condition, and ν was obtained at minimum deviation between measurements and simulations. For the five soils, we obtained an average ν of 3.5 (for stress transmitting from 0.1 to 0.7 m depth). This was only slightly different from $\nu = 3$ for which the elasticity theory-based classical solution of Boussinesq (1885) is satisfied. We noted that the estimated ν was strongly dependent on (i) the reliability of stress measurements, and (ii) the upper stress boundary condition used for simulations. Finite element simulations indicated that the transmission of vertical stresses in a layered soil is not appreciably different from that seen in a homogeneous soil unless very high differences in soil stiffness are considered. Our results highlight the importance of accurate stress readings and realistic upper model boundary conditions, and suggest that the actual stress transmission could be well predicted according to the theory of elasticity for the conditions investigated.

© 2014 Elsevier B.V. All rights reserved.

1. Introduction

The transmission of stress within a soil due to agricultural machinery is of major importance since the soil can undergo deformation due to stress, resulting in changes in the soil functions. A knowledge of stress transmission is needed, among others, for two purposes: first, in order to understand the relationships between cause (soil stress due to mechanical loading) and effect (changes in soil pore functioning); and second, to develop predictive models and decision support tools that can help land users prevent soil compaction.

Stress transmission in agricultural soil is typically modelled in relation to the problem of the normal loading of the surface of a homogeneous isotropic elastic halfspace by a concentrated normal force P , for which the analytical solution was obtained by Boussinesq (1885). The vertical normal stress distribution within the soil mass is given by:

$$\hat{\sigma}_z = \frac{3P}{2\pi} \frac{z^3}{r^5} \quad (1)$$

where $\hat{\sigma}_z$ is the simulated vertical soil stress, $r = (x^2 + y^2 + z^2)^{1/2}$ is the distance from the point of action of the point load P to the desired location (x, y, z) . In this paper, we shall deal only with vertical stresses, and therefore, only the equations for vertical stresses are presented. In agricultural soil mechanics the equation by Fröhlich (1934) is most often used, which allows alteration to the decay pattern of the vertical stress due to Boussinesq's solution

* Corresponding author at: Agroscope, Department of Natural Resources & Agriculture, Reckenholzstrasse 191, CH-8046 Zürich, Switzerland.
Tel.: +41 44 377 76 05; fax: +41 44 377 72 01.

E-mail address: thomas.keller@agroscope.admin.ch (T. Keller).

Table 1

Properties and initial conditions of the soils analyzed (mean values for 0.3–0.7 m depth). F_{wheel} , wheel load; P_{tyre} , tyre inflation pressure; Clay < 2 μm ; Silt 2–50 μm ; Sand 50–2000 μm ; ρ_0 , initial bulk density; w_0 , initial gravimetric water content; σ_{pc} , precompression stress.

Site	Reference ¹	F_{wheel} (kN)	P_{tyre} (kPa)	Clay (wt.%)	Silt (wt.%)	Sand (wt.%)	ρ_0 (Mg m^{-3})	w_0 (g g^{-1})	σ_{pc} (kPa)
Billeberga (SE)	1	86	100, 150, 250	30.6	40.2	29.2	1.68	0.189	92.3
Önnestad (SE)	2	82	90, 220	35.0	48.4	16.7	1.54	0.250	138.4
Strängnäs (SE)	1	32	180	61.0	30.7	8.3	1.39	0.332	129.9
Ultuna (SE)	3	11, 15, 33	70, 100, 150	60.6	23.8	15.7	1.40	0.311	73.0
Vallø (DK)	4	24	60	13.3	26.8	60.0	1.56	0.175	96.8

1: Keller and Arvidsson (2004); 2: Arvidsson et al. (2002); 3: Arvidsson and Keller (2007); 4: Keller et al. (unpublished data).

through the introduction of a “concentration factor”:

$$\hat{\sigma}_z = \frac{\nu P}{2\pi} \frac{z^\nu}{r^{\nu+2}} \quad (2)$$

where ν is the concentration factor (Fröhlich, 1934). For $\nu = 3$, Eq. (2) satisfies the solution based on the classical theory of elasticity (Boussinesq, 1885; Eq. (1)).

Stress transmission under agricultural vehicles is, however, not a point-load problem; instead, the load acts over an area (i.e. the tyre-soil or track-soil contact area). Linear elasticity allows superposition, and thus the stress at any depth, z , due to distributed normal loading at the soil surface can be calculated as follows: the contact area is divided into i small elements that each have an area A_i and a normal stress, σ_i , and carry a load $P_i = \sigma_i A_i$, which is treated as a point load. Disregarding horizontal stresses in the contact area, $\hat{\sigma}_z$ is then calculated as (Söhne, 1953):

$$\hat{\sigma}_z = \sum_{i=0}^{i=n} (\hat{\sigma}_z)_i = \sum_{i=0}^{i=n} \frac{\nu P_i}{2\pi} \frac{z_i^\nu}{r_i^{\nu+2}} \quad (3)$$

For a given surface load, $\hat{\sigma}_z$ at depth z becomes a sole function of ν (Eq. (3)).

The concentration factor was introduced because the rate of decay of the stress as predicted by the classical theory of elasticity (i.e., Eq. (1)) was found to be at variance with experimental observations of vertical stress distributions in soil (Söhne, 1953; Davis and Selvadurai, 1996). The discrepancy between the simulated and measured stress was ascribed to inaccurate model predictions, while measured stress values were assumed to be correct. However, measurements of stress in soil may be biased because embedded transducers do not read true stresses (Kirby, 1999; Berli et al., 2006a). Moreover, stress simulations, e.g. using Eq. (3), are sensitive to the stress boundary conditions at the surface (upper model boundary condition), i.e. the area over which the stress is applied and the distribution of the surface stresses (Keller and Lamandé, 2010).

The aim of this paper was to measure and simulate soil stress under defined loads. Measured stress was compared with simulated stress using Eq. (3), and the simulations obtained using Eq. (3) were also compared with finite element calculations. Moreover, the sensitivity of ν (Eq. (3)) to (i) the upper model boundary condition and (ii) stress readings (stress transducer estimates of the soil stress) was investigated.

2. Materials and methods

2.1. Measurements of vertical soil stress

The experimental data of measured vertical soil stress from wheeling experiments performed on five soils (13–66% clay; Table 1) were used. All fields (Table 1) were conventionally tilled, including annual mouldboard ploughing to a depth of about 0.25 m. The experiments were carried out in autumn before primary tillage, or in spring (i.e. about half a year after primary

tillage). Most experiments were performed with several wheel loads and/or tyre inflation pressures (Table 1). The driving speed was typically 2 m s^{-1} . The wheeling experiments reported here were carried out at a soil water content close to field capacity (Keller and Arvidsson, 2007). During wheeling experiments, the vertical stress was measured by installing probes (Fig. 1a) into the soil horizontally from a dug pit (Arvidsson and Andersson, 1997; Keller and Arvidsson, 2004) as shown in Fig. 1b. The stress was measured at three different depths, namely 0.3, 0.5 and 0.7 m. In this study, we used vertical stress measured below the centre of the loaded area.

The transducers used in this study over-predicted the vertical stress by 10% (Lamandé et al., 2014). Therefore, the transducer readings were corrected before further analysis and the vertical soil stress was assumed to be equal to 0.9 times the transducer-estimated stress (Lamandé et al., 2014).

Some of the wheeling experiments have already been reported elsewhere (Arvidsson et al., 2002; Keller and Arvidsson, 2004; Arvidsson and Keller, 2007). In the present study, we collated these data and analyzed them with respect to the stress transmission.

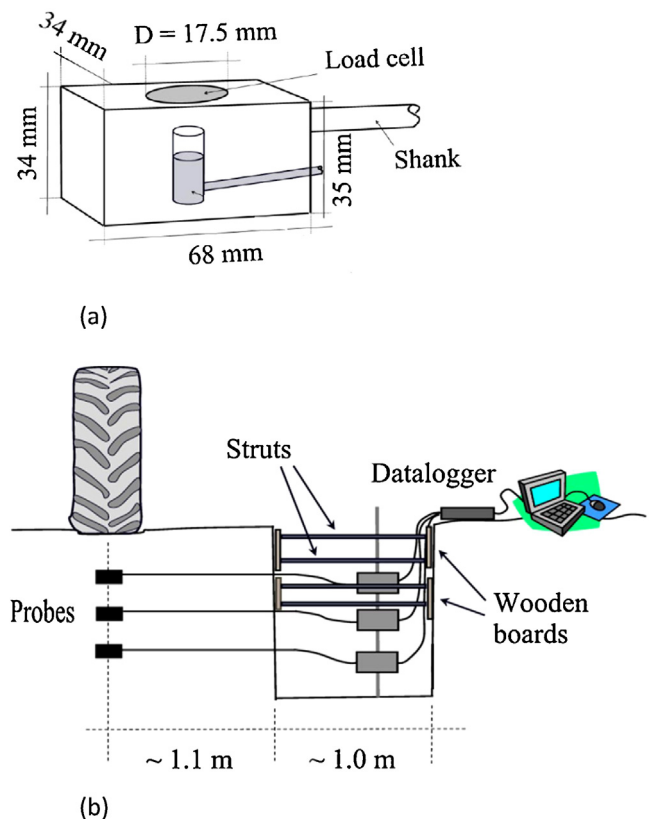


Fig. 1. (a) Probe (load cell and housing) used to measure vertical stress. (b) Experimental set-up for measurement of vertical stress at three depths. Source: from Keller and Arvidsson (2004).

2.2. Simulation of vertical soil stress

We simulated the vertical soil stress using Eq. (3) for the given situations and employing *SoilFlex* (Keller et al., 2007). The upper model boundary condition (i.e. the tyre-soil contact) was not measured during all the experiments listed in Table 1, so it was estimated from the tyre and loading characteristics using the model given by Keller (2005) as incorporated in *SoilFlex*. Because the model by Keller (2005) was based on measurements at 0.1 m depth (i.e. close to but not exactly at the tyre-soil contact), we used estimates from this model as input to Eq. (3) at the 0.1 m depth. That is, stress transmission was simulated from 0.1 m and below.

A subroutine was programmed in *SoilFlex* that yields the root mean squared error (RMSE) between the measured and simulated stress as a function of ν . The RMSE is given as:

$$RMSE = \sqrt{\frac{1}{n} \sum_{i=1}^n (\hat{\sigma}_z - \sigma_z)^2} \quad (4)$$

where n is the number of observations (here: measuring depths), $\hat{\sigma}_z$ is the predicted vertical stress, and σ_z is the measured vertical stress. For further analysis we used ν at the minimum RMSE. From the different loading situations on one soil (see Table 1), we calculated an average ν for each soil. This is justified because we could not find any noticeable influence of loading (wheel load, tyre inflation pressure) on ν (not shown). We also calculated the bias for each measuring depth, which is given as:

$$bias = (\hat{\sigma}_z - \sigma_z) \quad (5)$$

2.3. Sensitivity of the concentration factor to model input, stress readings, and transducer depth

The estimated ν is dependent on (i) the simulated stress, $\hat{\sigma}_z$, and (ii) the measured stress, σ_z (Eqs. (3) and (4)). The simulated stress at a given depth z and for a given value of ν is only dependent on the surface load distribution and on the area over which the load acts (Eq. (3)), i.e. on the upper stress boundary condition used for simulations. Therefore, it is important to analyze the sensitivity of ν to the surface stress boundary condition. In order to obtain ν , $\hat{\sigma}_z$ is compared with σ_z (Eqs. (3) and (4)), and hence, the estimated ν is dependent on the reliability of stress measurements. However, as mentioned previously, embedded stress transducers may not provide the true stress. Stress readings are influenced by a range of factors, including mechanical properties of soil, mechanical properties of the transducer, transducer dimensions; the interaction of these factors is complicated so that no simple relationships can be obtained (Weiler and Kulhawy, 1982; Kirby, 1999; Berli et al., 2006a). Therefore, it is of interest to study the sensitivity of ν to stress readings. Furthermore, comparisons between simulations and measurements and hence estimates of ν are influenced by the accuracy of the transducer depths.

The sensitivity of the simulated soil stress, and hence ν , to the upper model boundary condition was investigated by performing simulations using (i) the measured stress distribution at 0.1 m depth, i.e. near the tyre-soil contact, (ii) the estimated stress distribution as described above, and (iii) different commonly-used approximations of the tyre-soil contact stress distribution such as either the uniform or power-law stress distributions (Söhne, 1953).

The sensitivity of ν to stress readings was examined by comparing simulations with measurements where the stress readings were assumed to be (i) 10% overestimated or (ii) 10% underestimated as compared with (iii) a reference situation ("true" stress), which were the corrected transducer readings.

In addition, we investigated the sensitivity of ν to errors in stress transducer depths. For example, Keller et al. (2012) assumed that the probes were installed at the intended depth to an accuracy of ± 0.025 m. The roughness of the soil surface contributes to uncertainty in accurately measuring the depth. Moreover, the distance between the tyre-soil interface and the sensor depth changes during wheeling due to rut formation and soil displacement. We performed comparisons between simulations and measurements and associated estimates of ν for measuring depths ± 0.025 m, i.e. transducer depths of (i) 0.275, 0.475 and 0.675 m; (ii) 0.3, 0.5 and 0.7 m (i.e. the intended initial depths), and (iii) 0.325, 0.525 and 0.725 m.

2.4. Impact of data set (one-, two-, and three-dimensional vertical soil stress data) on the estimation of the concentration factor

The data set described in Section 2.1, consisted of one-dimensional data of vertical soil stress, i.e. maximum vertical stress at three different depths below the centre of a tyre.

Lamandé and Schjønning (2011a,b,c) measured the three-dimensional distribution of the vertical stress, i.e. vertical stress in the driving direction and perpendicular to the driving direction at three different depths. We revisited data of Lamandé and Schjønning (2011a,c) in order to investigate whether the estimate of ν would change when using (i) one-dimensional (as described in Section 2.1.) only, or (ii) two-dimensional (vertical stress in the driving direction at three different depths) or (iii) three-dimensional data (vertical stress in the driving direction and perpendicular to the driving direction at three different depths). The concentration factor was estimated for each case (i.e. one-, two-, or three-dimensional vertical soil stress data) using the procedure described in Section 2.2. We used the data set of vertical soil stress given in Lamandé and Schjønning (2011a,c), which were obtained on a silty clay loam soil from wheeling with a 800/50R34 tyre with 60 kN wheel load at a tyre inflation pressure of 100 kPa, three soil moisture conditions (\sim field capacity throughout the soil profile; drier than field capacity in the topsoil and \sim field capacity in the subsoil; and drier than field capacity in the whole soil profile; see Lamandé and Schjønning (2011c) for details) and two topsoil conditions (recently ploughed and consolidated topsoil, respectively; see Lamandé and Schjønning (2011a) for details).

2.5. Simulations using a finite element model

Additional simulations were carried out using finite element (FE) modelling within the framework of COMSOL Multiphysics Version 4.2. The aim was to investigate the influence of the elasto-plastic material properties, soil layers (topsoil over plough pan over subsoil) of different stiffness and strength, and the degree of anisotropy on the transmission of vertical stresses.

We applied a surface pressure, p_0 , of 250 kPa acting on a circular area of 0.5 m radius. The model was formulated as an axisymmetric problem (5 m radius, 5 m depth). The mesh (Fig. 2; 8246 elements) was vertically divided into three layers (plough layer: 0–0.25 m depth, plough pan: 0.25–0.35 m depth; subsoil: 0.35–5 m depth) for which different mechanical properties could be assigned. A bi-linear elasto-plastic model with isotropic strain hardening and associated flow rule was chosen as a constitutive relationship (for details on elasto-plasticity formulations on constitutive behaviour, see Shames and Cozzarelli, 1997 or Davis and Selvadurai, 2002). The assumption was that the soil deforms elastically (i.e. reversible) up to a yield stress beyond which deformation is plastic (i.e. irreversible). For simplicity, strain was assumed to increase linearly with increasing stress for both the elastic as well as the plastic range. Soil yield was estimated by using the von Mises yield criterion (von Mises, 1913). Soil

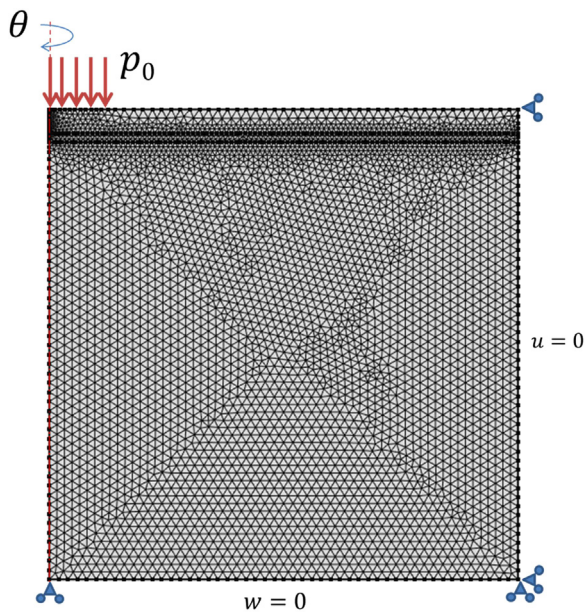


Fig. 2. Mesh, applied surface load, p_0 , and boundary conditions of the finite element model.

mechanical properties were adopted from the studies on ‘Ruckfeld’ silt loam soil (Berli et al., 2003, 2004) (Table 2). Young’s modulus, E , was calculated from oedometer test stress–strain curves according to Berli et al. (2006b). The isotropic tangent modulus was estimated as one-tenth of the Young’s modulus.

We first conducted a simulation for a linear-elastic, homogeneous, isotropic soil and compared this FE simulation with the analytical solution (Eq. (3) with $\nu = 3$). Then, more complexity was successively added to the model by introducing the elasto-plastic material law, and by introducing first two (topsoil, subsoil) and then three layers (topsoil, plough pan, subsoil) that were parameterized based on measurements on intact soil cores collected from an arable soil, as described above.

Finally, we made simulations that would allow us to investigate the impact on the transmission of σ_z with: (i) the topsoil to subsoil

modulus ratio, i.e. $E_{\text{topsoil}}/E_{\text{subsoil}}$, in a two-layer system (topsoil over subsoil, no plough pan); and (ii) the plough pan to subsoil modulus ratio, i.e. $E_{\text{plough-pan}}/E_{\text{subsoil}}$, and (iii) the elastic anisotropy of the plough pan, i.e. $E_{\text{subsoil_horizontal}}/E_{\text{subsoil_vertical}}$, in a three-layer system (topsoil over plough pan over subsoil). In all these simulations, only one parameter was changed and all other parameters were kept as given in Table 2: in (i) we increased E_{subsoil} , in (ii) we varied E_{subsoil} , and in (iii) we changed $E_{\text{subsoil_vertical}}$.

3. Results

3.1. Estimation of the concentration factor

The average ν per soil was in the range 2.8 to 4.4, with a mean value of 3.5 (coefficient of variation, C.V. = 19%) (see Table 3). The smallest value of ν (2.8) was obtained when a silty clay loam (‘Önnestad’) was loaded with a 82 kN wheel load. The highest value for ν was 4.4, obtained for loading a clay soil (‘Strängnäs’) with a 32 kN wheel load. The RMSE (Eq. (4)) was in the range 1.8–19.2 kPa, with a mean value of 13.3 kPa. The average bias (Eq. (5)) was negative (–8.4 kPa; i.e. an underestimation of stress) at the 0.3 m depth (i.e. the uppermost sensor depth), positive (11.0 kPa; i.e. an overestimation of stress) at the 0.5 m depth (i.e. the intermediate sensor depth), and close to zero (–2.8 kPa) at a depth of 0.7 m (i.e. the deepest sensor location). The data are summarized in Table 3. Both the soil texture and loading (wheel load, tyre inflation pressure) had no effect on ν ($p > 0.05$; not shown). Similarly, Pytka (2005) and Zink et al. (2010) found no impact of soil texture on stress transmission.

The average value for ν of 3.5 only differs slightly from $\nu = 3$; when $\nu = 3$, Eqs. (2) and (3) satisfy the elastic theory of Boussinesq (1885) (Eq. (1)). For this reason, additional simulations were conducted with $\nu = 3$ for all the loadings given in Table 1; this resulted in the RMSE being somewhat higher, and the bias slightly more negative at the 0.3 and the 0.7 m depths but smaller at the 0.5 m depth (Table 4) as compared with the simulations with variable ν as described above (Table 3).

The RMSE reported in Tables 3 and 4 may be compared with the standard deviation of the stress measurements, which was on

Table 2
Mechanical properties of “Ruckfeld” silt loam soil (Berli et al., 2003, 2004).

	Topsoil (0–0.25 m)	Plough pan (0.25–0.35 m)	Subsoil (0.35–5 m)
Bulk density (kg m^{-3})	1.3×10^3	1.5×10^3 (b), 1.6×10^3 (c,d)	1.5×10^3
Young’s modulus (kPa)	1500	3×10^3 (b), 5×10^3 (c), 5×10^5 (d)	3×10^3
Poisson’s ratio (–)	0.33	0.33	0.33
Precompression stress (kPa)	40	80 (b), 150 (c), 300 (d)	80
Isotropic tangent modulus (kPa)	150	300 (b), 500 (c), 5×10^4 (d)	300

Note that indices (b), (c) and (d) correspond to the notation on the stress calculations for the different “layering scenarios” shown in Fig. 6. Hypothetical values in italic. (b) Same mechanical properties for plough pan and subsoil; (c) Plough pan according to the measurements by Berli et al. (2003), Berli et al. (2004); (d) Plough pan with twice the precompression stress and 100 times the stiffness of (c).

Table 3
Estimated concentration factor (ν), root mean squared error (RMSE; Eq. (4)) and bias (Eq. (5)) for the loading conditions and soils described in Table 1.

Site	ν		RMSE (kPa) [‡]	Bias (kPa) [‡]		
	Range [†]	Mean		Mean	0.3 m	0.5 m
Billeberga (SE)	2.7–3.6	3.3	15.1	–0.8	16.5	–19.5
Önnestad (SE)	2.3–3.2	2.8	18.4	–3.0	10.7	–9.7
Strängnäs (SE)	4.4	4.4	1.8	1.8	–2.1	–1.3
Ultuna (SE)	2.2–3.9	3.1	12.0	–13.2	15.1	3.2
Vallø (DK)	3.9	3.9	19.2	–26.9	14.6	13.1
Mean		3.5	13.3	–8.4	11.0	–2.8

[†] For the different loading conditions given in Table 1.

[‡] Average per soil.

Table 4

Root mean squared error (RMSE; Eq. (4)) and bias (Eq. (5)) for the loading conditions and soils described in Table 1 when using a concentration factor (ν) of 3 for all simulations.

Site	ν	RMSE (kPa) [†]	Bias (kPa) [†]		
		Mean	0.3 m	0.5 m	0.7 m
Billeberga (SE)	3	18.1	-7.0	10.1	-24.5
Önnestad (SE)	3	21.7	2.2	16.6	-5.1
Strängnäs (SE)	3	19.7	-21.6	-22.1	-14.4
Ultuna (SE)	3	14.1	-12.7	14.5	2.6
Vallø (DK)	3	21.1	-35.2	6.2	7.3
Mean	3	18.9	-14.9	5.1	-6.8

[†] Average per soil.

average 28.4 kPa for the measurements reported here (not shown); i.e., the standard deviation of the measurements was larger than the RMSE.

For the soil conditions reported here (Table 1), ν would typically be given a value of 6 (Söhne, 1953). Simulations with $\nu = 6$ yielded an average RMSE of 32.9 kPa, i.e. about twice as large as the RMSE for simulations with variable ν (Table 3) or $\nu = 3$ (Table 4), and the bias was positive (i.e. the stress was overestimated) at all depths in the range 18.0–43.0 kPa, which is considerably higher than the bias presented in Tables 3 and 4.

3.2. Sensitivity of the concentration factor to the data set when using one-, two-, or three-dimensional vertical soil stress data

We found that the estimate of ν differed between the different data sets, but that there was no conclusive overall trend of increasing or decreasing ν when moving from one-, to two- or three-dimensional data (not shown). There appeared to be an increase in the estimated ν for weak soil (moisture content at about field capacity and recently ploughed topsoil) when using two-dimensional instead of one-dimensional data, but ν decreased again when three-dimensional data were used. For these soil conditions, ν was on average 13% larger when estimated from three-dimensional data than when obtained from one-dimensional data. No difference in ν between one- and two-dimensional data was observed for the two slightly drier soil conditions, while ν was smaller when considering three-dimensional data. For all situations analyzed here, ν was on average 4% smaller when three-dimensional data were used as compared with estimates of ν based on one-dimensional data.

3.3. Sensitivity of the concentration factor to the surface stress boundary condition

The sensitivity of ν to the surface stress boundary condition (upper model boundary condition) was evaluated using the 'Billeberga' soil and one loading situation (86 kN wheel load, 150 kPa tyre inflation pressure) (Table 1), because the measured stress distribution at the 0.1 m depth was available for this loading condition (Keller and Arvidsson, 2004). The various surface stress boundary conditions are shown in Fig. 3 and the associated stress simulations in Fig. 4 while the estimated ν and associated RMSE and bias are summarized in Table 5. It is important to note that the applied load is identical for the various surface stress boundary conditions used for the simulations that are shown in Fig. 3.

We estimated $\nu = 3.6$ for the simulations with a stress distribution that was estimated using Keller's model (2005). If, on the other hand, the measured stress distribution at the 0.1 m depth was used (Keller and Arvidsson, 2004), a value for ν of 3.8 was obtained, which is only slightly different from the ν estimate in the former simulation. The RMSE and the bias of the two simulations were very similar (Table 5). Furthermore, both the simulations were run assuming an elliptical contact area and either

a uniform or a power-law distribution (using either a power of 1.5 or 2) of the contact stress. These shapes for the (theoretical) stress distributions are often used as approximations of the real stress distribution at the tyre-soil contact (Söhne, 1953; Johnson and Burt, 1990). The estimates of ν were 5.0 (uniform stress distribution), 3.2 (power-law distribution with a power of 1.5), and 2.5 (power-law distribution with a power of 2, i.e. parabolic distribution), see Table 5. For the uniform distribution, the RMSE was 29.7 kPa, which is about twice that for the simulations using either measured (RMSE = 14.0 kPa) or model-estimated stress distribution (RMSE = 13.3 kPa), and the bias was highly negative at the 0.3 m depth (-48.7 kPa) (Table 5). The parabolic stress distribution resulted in a positive bias at a depth of 0.3 m (9.5 kPa) with an RMSE of 17.9 kPa. For the case of the power-law stress distribution with a power of 1.5, the RMSE and the bias were similar to the simulations with the measured or model-estimated stress distributions (Table 5).

3.4. Sensitivity of the concentration factor to stress readings

The sensitivity of ν to stress readings was investigated by comparing estimates for ν where the stress readings were assumed to be (i) 10% overestimated or (ii) 10% underestimated as compared with (iii) a reference situation ("true" stress = corrected transducer readings). Loading with a 1050/50R32 tyre (wheel load 86 kN; tyre inflation pressure 150 kPa) on a loam soil was used as an illustrative example.

When using stresses that were 10% overestimated, the average ν was 4.5, i.e. 21% higher than for the reference situation ($\nu = 3.6$) (Fig. 5). On the other hand, if the stress was 10% lower than the assumed true stress, then we obtained an average value for ν of 2.9, which is 17% lower than when using the correct estimates of stress (Fig. 5). Hence, an uncertainty in the stress readings of $\pm 10\%$ resulted in an uncertainty in the value of ν of roughly $\pm 20\%$.

3.5. Sensitivity of the concentration factor to transducer depths

We used the same illustrative example as described in the previous section, and compared simulations with measurements by assuming the transducer depths to be either (i) 0.275, 0.475 and 0.675 m; (ii) 0.3, 0.5 and 0.7 m (i.e. the intended initial depths), or (iii) 0.325, 0.525 and 0.725 m; i.e. intended initial measuring depths ± 0.025 m. The associated estimated ν was (i) 3.2, (ii) 3.6, and (iii) 4.0, respectively, i.e. $3.6 \pm 10\%$. Therefore, uncertainty in the measuring depth of only a few centimetres, which could be due to factors such as the installation, soil surface roughness or rut formation, will result in an uncertainty of ν of $\pm 10\%$.

3.6. Effects of soil layering on stress transmission using finite element model simulations

Fig. 6a compares the results of FEM calculations with the exact analytical solution based on Boussinesq's (1885) equation

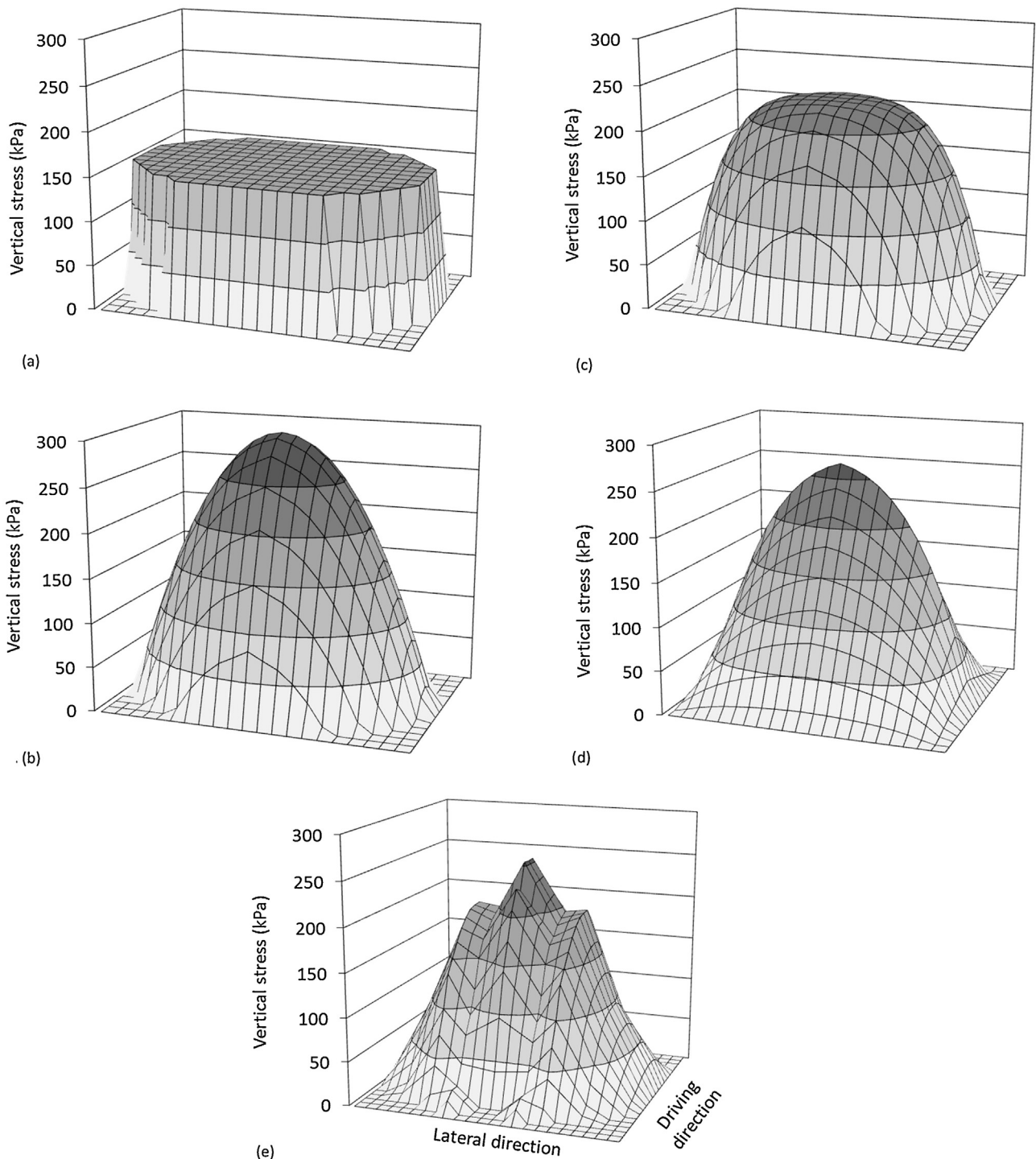


Fig. 3. Upper model boundary condition (i.e. contact area and contact stress distribution) used for the simulations shown in Fig. 4, for a 1050/50R32 tyre (wheel load: 86 kN; tyre inflation pressure: 150 kPa). (a) Uniform stress distribution, (b) parabolic stress distribution, (c) power-law stress distribution with a power of 1.5, (d) estimated stress distribution using the model of Keller (2005), and (e) measured stress distribution.

providing a calibration of the FE model for a linear-elastic, homogeneous, isotropic soil. Fig. 6b shows a comparison of the analytic solution from Fig. 6a with a FEM calculation for an elasto-plastic soil consisting of a plough layer (0–0.25 m depth) over a subsoil (0.25–5 m depth) without a plough pan (for details of the material properties, see Table 2). For the loads applied, plastic deformation occurred in the topsoil and the upper part of the subsoil, while the vertical stress profiles were very similar for elastic and elasto-plastic soils. It should also be noted that the layering (soft plough layer over stiffer subsoil, Table 2) had no

influence on the vertical stress profile. Fig. 6c shows similar calculations as in Fig. 6b but considers a 0.1 m thick plough pan in the 0.25–0.35 m depth between the plough layer and the subsoil. Values for plough pan Young's modulus ($E = 5000$ kPa) and precompression stress (130 kPa at 60 hPa soil water suction) were derived from actual measurements for 'Ruckfeld' soil (Berli et al., 2003, 2004). The vertical stress profiles in Fig. 6c are very similar to those seen in Fig. 6a and b, indicating that a plough pan of "normal" stiffness and 0.1 m thickness has little to no effect on the vertical stress profile. Fig. 6d gives similar calculations as in Fig. 6c but here

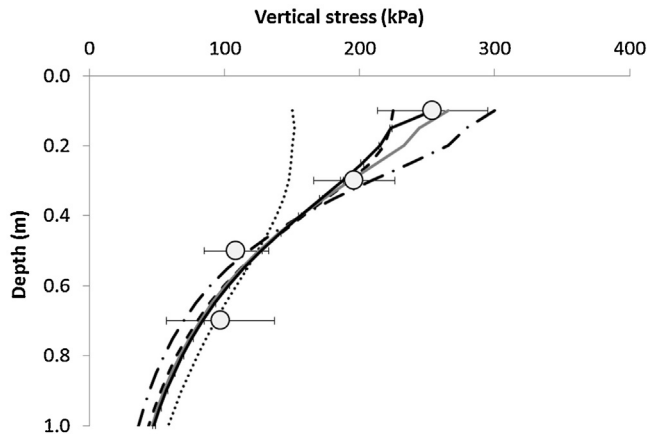


Fig. 4. Measured (circles) and simulated vertical stress beneath the centre of a wheel with a 1050/50R32 tyre with a load of 86 kN and an inflation pressure of 150 kPa using uniform stress (dotted curve; $\nu = 5.0$, RMSE = 29.7), parabolic distribution (chain-dotted curve; $\nu = 2.5$, RMSE = 17.9), power-law distribution with a power of 1.5 (dashed curve; $\nu = 3.2$, RMSE = 14.3), calculated stress distribution with the model of Keller (2005) (grey curve; $\nu = 3.6$, RMSE = 13.3) and measured stress distribution (black curve; $\nu = 3.8$, RMSE = 14.0) as model input at 0.1 m depth. Error bars indicate standard deviation. See text and Table 5 for details.

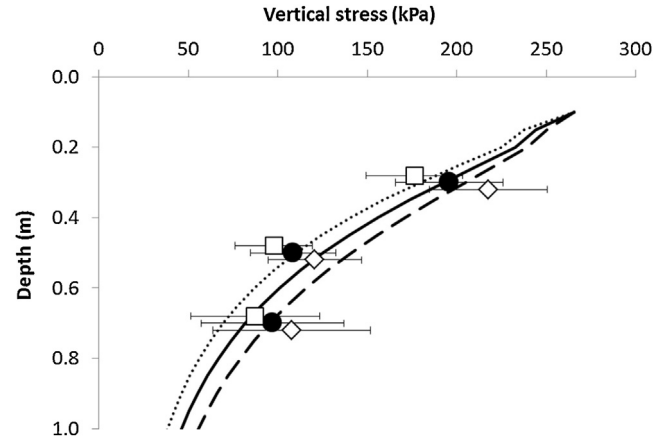


Fig. 5. Measured and simulated vertical stress as a function of depth beneath the centre of a 1050/50R32 tyre (wheel load 86 kN, tyre inflation pressure 150 kPa). The concentration factor (Eq. (3)) is fitted to (i) the assumed true soil stress (measurements: circles; simulations: solid curve; $\nu = 3.6$), (ii) a 10%-underestimated soil stress (measurements: squares; simulations: dotted curve; $\nu = 2.9$), and (iii) a 10%-overestimated soil stress (measurements: rhombi; simulations: dashed curve; $\nu = 4.5$). Error bars indicate standard deviation. Note that the measured soil stress of (ii) and (iii) is slightly displaced for better readability. See text for details.

Table 5

Estimated concentration factor (ν), root mean squared error (RMSE; Eq. (4)) and bias (Eq. (5)) for the simulations shown in Fig. 4. The different stress distributions are shown in Fig. 3.

Shape of contact area	Measured	Super ellipse	Ellipse		
			Uniform	Power-law ($k = 1.5^{\dagger}$)	Power-law ($k = 2^{\dagger}$)
Stress distribution	Measured	Keller (2005)			
ν at RMSE = min	3.8	3.6	5.0	3.2	2.5
RMSE (kPa)	14.0	13.3	29.7	14.3	17.9
Bias (kPa)					
At 30 cm	-8.8	-3.1	-48.7	-3.4	9.5
At 50 cm	18.4	16.9	16.0	17.4	7.0
At 70 cm	-13.3	-15.3	-3.6	-17.2	-28.6

[†] k, power.

the plough pan is 100 times stiffer (Young's modulus of 500 MPa instead of 5 MPa) and has a considerably higher precompression stress (300 kPa rather than 130 kPa). For the case of a very stiff plough pan, the vertical stress within and immediately below the plough pan is decreased compared with the stress profiles from Fig. 6a to c. Although theoretically possible, a Young's modulus of 0.5 GPa seems to be unrealistically high for a "soft" porous material such as agricultural soil at field capacity. The precompression stress value of 300 kPa was chosen so that the plough pan did not yield under the given load.

The impact of a (stiff) plough pan on the transmission of vertical stress was more closely investigated and the results are presented in Fig. 7. The vertical stress is reduced in the plough pan, but only if the $E_{\text{plough-pan}}/E_{\text{subsoil}}$ is very large. Note that for the simulations presented, E_{topsoil} was similar to E_{subsoil} (Table 2). If the modulus of the plough pan is one order of magnitude larger than that of the subsoil (which is already quite significant, cf. the measurements in a silt loam soil at field capacity as presented in Table 2), there is hardly any impact on the stress pattern (Fig. 7a) and the reduction in σ_z at 0.4 m depth (i.e. directly below the plough pan) is less than 5% (Fig. 7b). It seems that the stress reduction becomes stronger when $E_{\text{plough-pan}}/E_{\text{subsoil}}$ is larger than about 20 (Fig. 7b). When the plough pan is 100 times stiffer than the subsoil, the reduction in σ_z is 26% and 20% at 0.4 and 0.7 m depth, respectively.

Anisotropy in the plough pan may be a realistic scenario, and often a platy soil structure is observed in compacted soil layers (e.g. Horn, 2003; Pagliai et al., 2003; Boizard et al., 2013). Fig. 8 shows that anisotropy, i.e. $E_{\text{plough-pan_vertical}}/E_{\text{plough-pan_horizontal}} \neq 1$,

affects the vertical stress in the soil profile, but the impact does not seem to be large. We note that our simulated anisotropy effects are potentially due to changes in the magnitude of the stiffness, but these changes were marginal. Moreover, in order to truly distill the anisotropic effects, empirical data would be required in order to quantify the 21 elastic components of the stiffness matrix (see e.g. Davis and Selvadurai, 1996) for the boundary conditions prescribed in this paper.

It should be noted that the simulations with a plough pan were made for a 0.1 m thick plough pan. The impact of layer thickness on stress transmission is not easily quantified, because the layer stiffness decreases with increasing layer thickness if E is kept constant. We found negligible effects of plough pan thickness on stress transmission when $E_{\text{plough-pan}}/E_{\text{subsoil}}$ was smaller than 10 (simulations not shown); hence, for realistic ratios of $E_{\text{plough-pan}}/E_{\text{subsoil}}$ the stress transmission was not appreciably affected by the thickness of the plough pan. For large ratios of $E_{\text{plough-pan}}/E_{\text{subsoil}}$ (e.g. $E_{\text{plough-pan}}/E_{\text{subsoil}} = 1000$) the stress within the plough pan initially decreased when increasing the thickness of the plough pan, but then increased again with further increasing thickness of the plough pan because the plough pan stiffness decreased as explained above (simulations not shown). When increasing the plough pan thickness to very large values the stress transmission approached that of the two layer system (topsoil over subsoil) as presented below.

Simulations in a two-layered soil showed that the vertical stress increases as the difference in Young's modulus between the two layers increases, i.e. σ_z increases with decreasing $E_{\text{topsoil}}/E_{\text{subsoil}}$

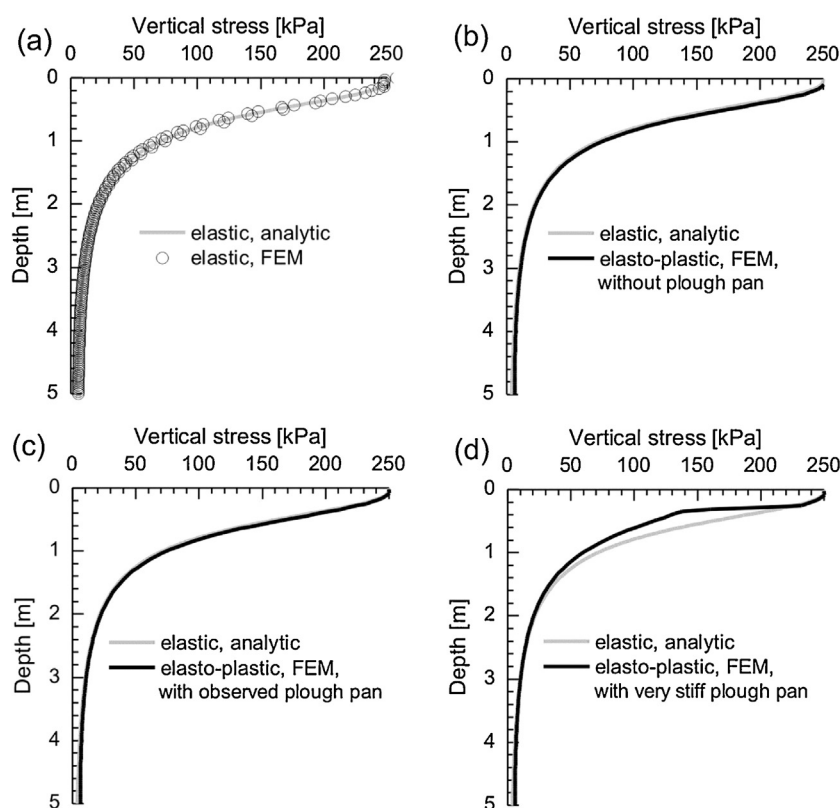


Fig. 6. Calculated vertical stress as a function of depth. (a) Comparison of the analytical solution with the finite element model (FEM) calculations for a linear-elastic, homogeneous, isotropic soil. (b) Comparison of the analytical solution from (a) with FEM calculations for an elasto-plastic soil consisting of a topsoil (0–0.25 m depth) over a subsoil (0.25–5 m depth) without a plough pan. (c) Comparison of the analytical solution from (a) with FEM calculations for an elasto-plastic soil consisting of a soft topsoil (0–0.25 m depth), a plough pan with usually observed stiffness (0.25–0.35 m depth) over a subsoil (0.35–5 m depth). (d) Comparison of the analytical solution from (a) with FEM calculations for an elasto-plastic soil consisting of a topsoil (0–0.25 m depth), a very stiff plough pan [0.25–0.35 m depth, 100 times the stiffness of the plough pan in (c)] over a subsoil (0.35–5 m depth).

(Fig. 9). Our simulations agree with stress decay patterns in two-layer systems presented in Poulus and Davis (1974). The simulation with $E_{\text{topsoil}}/E_{\text{subsoil}} = 10^{-100}$ represents a subsoil that is nearly an ideal rigid body. It is seen from Fig. 9 that the effect of layer differences is limited and converges. The maximum difference in σ_z/p_0 between the simulations with $E_{\text{topsoil}}/E_{\text{subsoil}} = 0.5$ and $E_{\text{topsoil}}/E_{\text{subsoil}} = 1$ was 0.06 (Fig. 9), which for $p_0 = 250$ kPa corresponds to a maximum difference in σ_z of only 14.0 kPa, i.e. an insignificant difference (cf. Fig. 6b). Comparing the reference simulation ($E_{\text{topsoil}}/E_{\text{subsoil}} = 1$) with the simulation with $E_{\text{topsoil}}/E_{\text{subsoil}} = 10^{-100}$, the maximum difference in σ_z/p_0 was 0.15 (Fig. 9) that corresponds to 37.3 kPa for $p_0 = 250$ kPa. It is interesting that a change in E_{subsoil} (while keeping E_{topsoil} constant) affects the stress in the topsoil. This is because the topsoil “sees” the subsoil and the topsoil-subsoil interface acts similar to a boundary when $E_{\text{topsoil}}/E_{\text{subsoil}}$ becomes small. We estimated ν for the vertical stress obtained with $E_{\text{topsoil}}/E_{\text{subsoil}} = 10^{-100}$ using the procedure described in Section 2.2. In this case, the FE simulation was considered the “measured” stress, and ν was estimated from “measurements” at 0.3, 0.5 and 0.7 m depth as was done for the data described in Section 2.1. We obtained a value for ν of 4.5.

4. Discussion

Fröhlich’s model, including ν , is widely used in agricultural soil mechanics, usually in the form of Eq. (3) (Keller and Lamandé, 2010). Despite the wide use of this model, little is known about ν in terms of how it varies with soil type and conditions.

Fröhlich (1934) made the assumption that forces are transmitted along straight lines through the soil. The effect of ν can be seen

as analogous to the transmission of light in a vacuum or air from an infinitely small light source. Similar to the focusing effect of a lens for light, we could imagine that the soil, depending on its properties, will have a focusing effect on the ‘stress beams’, which is expressed by ν . Depending on the soil properties, stress beams were considered to be more or less focused towards the centre line of the point load. Generally, the concentration factor is regarded an empirical parameter that is needed because soil deviates from an elastic, homogeneous, isotropic material (e.g. Söhne, 1953). It is commonly accepted that ν increases with a decrease in soil strength (Söhne, 1953; Horn, 1990). According to Horn (1990), ν is not only influenced by soil properties and conditions, but is also affected by the applied load. Results of Lamandé et al. (2007) indicate that ν increases with increasing soil deformation. Söhne (1953) suggested that ν takes values of 4, 5 and 6 for hard, firm and soft soil, respectively, but values for ν in the range 0.6–14.3 are found in the literature (Dexter et al., 1988; Horn, 1990; Ram, 1984; Lamandé et al., 2007; Keller and Lamandé, 2010; Lamandé et al., 2011a,b,c).

However, as shown in this paper, the estimation of ν is strongly dependent on the reliability of the stress measurements, the accuracy of the transducer depths, and the upper stress boundary condition used for the simulations. Söhne (1953) mentioned the tyre-soil stress distribution and the accuracy of stress measurements as potential sources of errors in his studies.

The reliability of the stress transducers, i.e. the relation between the measured stress and actual/true soil stress, is influenced by a range of factors including the transducer dimensions and the mechanical properties of the transducer in relation to those of its surrounding soil (Weiler and Kulhawy, 1982; Kirby, 1999). The

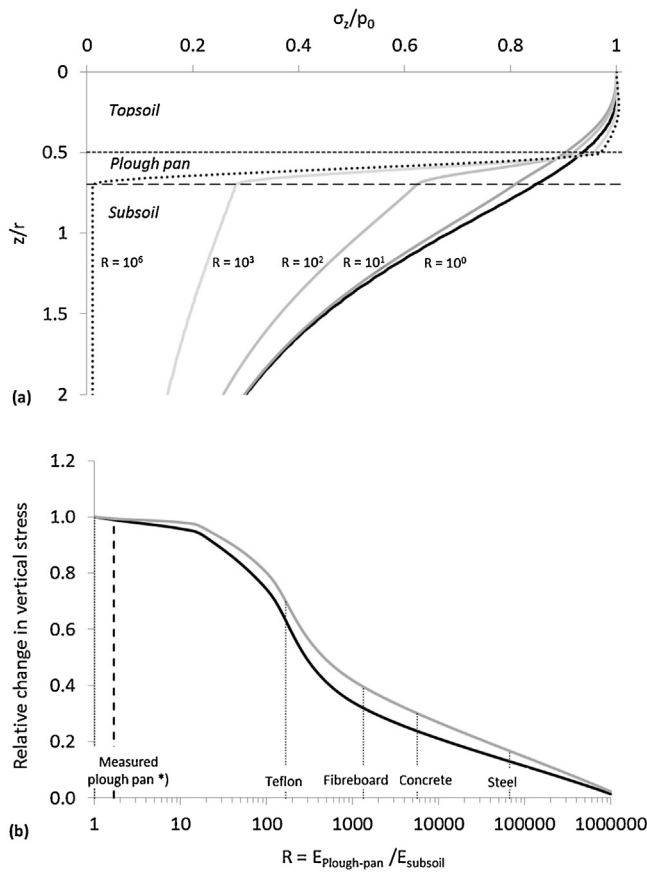


Fig. 7. Impact of plough pan stiffness of 0.1 m thickness on the transmission of vertical stress. (a) Relative vertical stress, σ_z/p_0 (where σ_z is the vertical stress and p_0 is the applied surface pressure), vs. relative depth, z/r (z is the soil depth and r is the radius of the circular region over which the load is applied), for different plough pan to subsoil modulus ratios, $R = E_{\text{plough-pan}}/E_{\text{subsoil}}$. (b) Relative change in vertical stress at 0.4 m (grey curve) and 0.7 m depth (black curve) as a function of $R = E_{\text{plough-pan}}/E_{\text{subsoil}}$. The properties of the plough pan as measured by Berli et al. (2003), Berli et al. (2004) resulted in $R = 1.67$. The corresponding R for a number of materials is indicated in the figure (e.g. $E_{\text{plough-pan}} = E_{\text{fibreboard}}$ would result in $R = 1330$, $E_{\text{plough-pan}} = E_{\text{concrete}}$ would result in $R = 5660$).

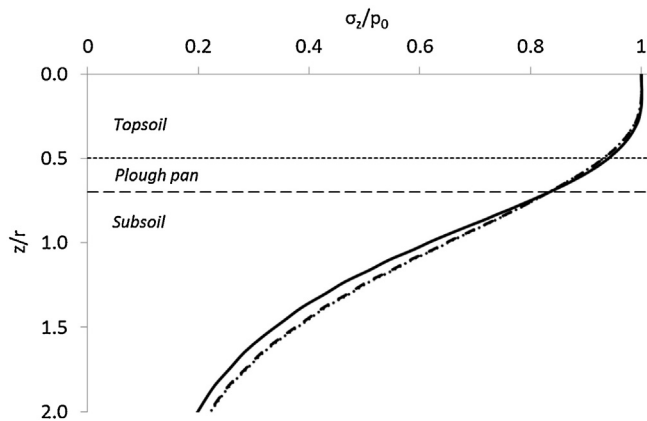


Fig. 8. Effect of elastic anisotropy of the plough pan on the transmission of vertical stress. The plough pan was 0.1 m thick, and anisotropy is expressed as $FA = E_{\text{plough-pan_vertical}}/E_{\text{plough-pan_horizontal}}$. Solid curve: $FA = 1$; dashed curve: $FA = 0.1$; and dotted curve: $FA = 0.01$. The graph shows relative vertical stress, σ_z/p_0 (where σ_z is the vertical stress and p_0 is the applied surface pressure), vs. relative depth, z/r (z is the soil depth and r is the radius of the circular region over which the load is applied).

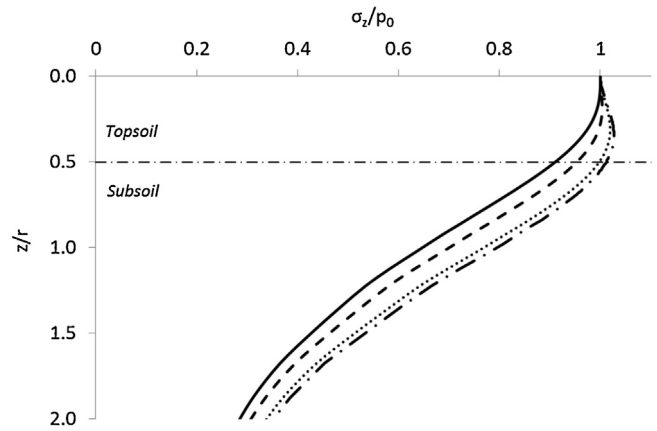


Fig. 9. Transmission of vertical stress as influenced by the difference in topsoil to subsoil modulus ratio, expressed as $T = E_{\text{topsoil}}/E_{\text{subsoil}}$. Solid curve: $T = 1$; dashed curve: $T = 0.5$; dotted curve: $T = 0.1$; and chain curve: $T = 10^{-100}$. The graph shows relative vertical stress, σ_z/p_0 (where σ_z is the vertical stress and p_0 is the applied surface pressure), vs. relative depth, z/r (z is the soil depth and r is the radius of the circular region over which the load is applied).

interaction of the different factors affecting the stress readings is complicated, and therefore, there is no general means of correcting them (Kirby, 1999). Based on field measurements we found that the transducers used here for vertical stress measurements overestimate the true vertical stress by approximately 10% (Lamandé et al., 2014). This value of 10% is within the range of the modelling results for vertical transducers reported by Kirby (1999). We have shown in this paper that an uncertainty of $\pm 10\%$ in the stress measurements accounts for an error in ν of about $\pm 20\%$ (Section 3.4). In other words, any estimation of ν is erroneous if the reliability of stress measurements (i.e. the ratio of transducer-estimated stress to true soil stress) is unknown. This was also acknowledged by Söhne (1953), who estimated that the error of stress measurements was within 25%. It is therefore extremely important to know the ratio of the stress transducer reading to the true soil stress when making any inference about the absolute stress values (Kirby, 1999), as well as for any comparison of the measured stress values with simulations (as used here). An uncertainty in the stress readings of the order of 10% seems relatively small, considering the many factors that influence the stresses estimated by transducers (Kirby, 1999). Kirby (1999) identified that a zone of disturbance around the stress transducer, e.g. due to transducer installation, would be one of the main factors contributing to either an overestimation or underestimation of the true stress by the transducer. The mechanical properties of the soil had a relatively small impact on transducer readings (Kirby, 1999), probably because the stiffness of the transducers is orders of magnitude larger than that of the soil. In this study, we always used the same installation procedure (cf. Section 2.1), and hence, the potential impact on transducer readings would be similar for all measuring depths and on all soils. Furthermore, soil moisture conditions were (i) similar for all soils, and (ii) similar to those during the calibration of the stress transducers in the field (Lamandé et al., 2014) that was applied in this study. We acknowledge that soil deformations are generally larger at the 0.3 m depth than the 0.7 m depth, and since deformation can influence stress readings (Kirby, 1999), the ratio of transducer-estimated stress to soil stress may not have been constant within a soil profile during loading, although the measured residual vertical strain was generally small (in the range 0–0.02, see Keller et al., 2012).

Another source of error associated with stress readings is the measuring depth. Errors in measuring depth arise from the installation (the intended measuring depth deviates from the true measuring depth), and from the roughness of the soil surface.

Furthermore, the vertical distance between the tyre-soil interface and the stress transducer will become smaller during loading due to rut depth formation and soil displacement. Typically, rut depths are a few centimetres (e.g. Défossez et al., 2003; Keller et al., 2007) and permanent vertical displacements in the subsoil (i.e. at depths greater than about 0.25 m) a few millimetres (Arvidsson et al., 2002; Keller et al., 2007; Lamandé et al., 2007). The error in estimating ν due to these measuring depth uncertainties may be of the order of magnitude of 10% (see Section 3.5).

The upper model boundary condition includes the magnitude and distribution (shape) of stress applied at the soil surface (e.g. the stress distribution at the tyre-soil contact area), and the area over which the load is applied (e.g. the tyre-soil contact area), and forms the input into Eq. (3). As shown by Keller (2005), the upper model boundary condition is of paramount importance to accurately predict stress transmission in soil. Unfortunately, the surface stress boundary condition is (i) typically not known a priori, and (ii) governed by a complicated interaction of tyre and soil properties (Keller and Lamandé, 2010). In this paper, we show that the estimate of ν varies greatly (e.g. between 2 and 5 for the example presented, see Section 3.3.) when different stress distributions (but always with the same load) are applied at the soil surface. The model by Keller (2005) used here generally provides good estimates of the real size and shape of the tyre-soil contact area and of the real distribution of vertical stresses within the contact area; however, model estimates may differ significantly from the real values for a specific tyre or a specific tyre-loading combination (Keller, 2005). The tyres and loading characteristics used in this study were within the range of tyres and loadings used by Keller (2005) and some of the tyre dimensions and tyre-loading combinations used here were explicitly employed in the model development by Keller (2005). Furthermore, the soil moisture conditions in our study were similar to those in Keller (2005). Hence, there is a good basis to assume that our estimates of the upper stress boundary condition were realistic. Nevertheless, deviations to the real tyre-soil contact properties are inevitable, and this introduced some error in our estimates of ν .

For the analyses discussed above, we estimated ν based on one-dimensional data of vertical soil stress (maximum stress at three different depths below the centre of a tyre). Using data from Lamandé and Schjøning (2011a,c) we found that ν differed slightly when using one-dimensional (as described), two-dimensional (vertical stress in driving direction at three different depths below the centreline of a tyre) or three-dimensional data (vertical stress in driving direction and perpendicular to driving direction at three different depths) for the different data sets, but that there was no overall trend of increasing or decreasing ν when moving from one-, to two- or three-dimensional data. Nevertheless, ν estimated from three-dimensional data was different from ν based on one-dimensional data, and therefore, we suggest that this needs further attention.

Based on this, the question is raised as to whether a concentration factor is needed since the classical Boussinesq solution (Eq. (1)) is insufficient to represent stress transmission in soil (Fröhlich, 1934), or whether a concentration factor was introduced because the measurements and surface stress boundary conditions were inaccurate (Davis and Selvadurai, 1996). It is interesting to note that when accounting for realistic upper model boundary conditions and accurate stress measurements, the average value for the estimated ν of 3.5 found here was not significantly different from $\nu = 3$ (i.e. the classical Boussinesq solution) for the conditions investigated in this paper. This implies that the stress transmission could indeed be described by the elasticity theory, i.e. by the classical Boussinesq solution (Eq. (1)), suggesting that the concentration factor may have been introduced due to measurement errors and inaccurate upper stress boundary

conditions. We are aware that our observations are limited to the loading and soil conditions investigated in this paper (Table 1).

Selvadurai (2013) observed that the solution provided by Fröhlich (1934) satisfied (i) the equations of static equilibrium, globally and locally, (ii) the traction boundary conditions on the free surface, (iii) the regularity in the decay of stress and displacement fields applicable to semi-infinite domains (i.e. decay of energy transfer), (iv) the equations of elasticity applicable to a homogeneous incompressible elastic material, but (v) violated the Beltrami-Michell equations of compatibility (Selvadurai, 2000) applicable to classical elastic continua, except when $\nu = 3$, which corresponds to Boussinesq's classical solution. The consequences of violating the compatibility conditions results in a non-unique evaluation of the displacement fields from the four linear partial differential equations applicable to a state of axial symmetry.

Obviously, agricultural soil is neither homogeneous nor completely elastic, and therefore, the assumptions on which the classical Boussinesq solution (Eq. (1)) is based are violated. However, elastic solutions may provide satisfactory approximations well beyond the range of small-deformation, linear-elastic material behaviour (Berli et al., 2006b). Furthermore, results of FEM simulations (Figs. 6 and 7) indicate that for a layered soil (topsoil over plough pan over subsoil) the transmission of vertical stresses is not appreciably different from that seen in a homogeneous soil unless unrealistically high differences in stiffness are considered. Similarly, a difference in Young's modulus between topsoil and subsoil increases the vertical soil stress (Fig. 9), but the simulated effect was limited. Nevertheless, the simulation results presented here need to be validated against field measurements. It is noteworthy to reiterate that the transmission of vertical stress is not dependent upon the Poisson's ratio (Boussinesq, 1885). Further, we recall that Fröhlich (1934) associated the concentration factor with anisotropy, as compared with isotropy that is assumed in the Boussinesq solution. Little is known on anisotropy of mechanical properties of arable soils. Peth et al. (2006) found a slight anisotropy (with higher values in the vertical direction) in precompression stress and cohesion on a clayey silt Stagnic Luvisols derived from loess soil, but Dörner and Horn (2009), investigating a sandy loam Stagnic Luvisols derived from glacial till, reported isotropic soil shear properties while soil pore transport functions (hydraulic conductivity, air permeability) were more anisotropic. Our simulations show that anisotropy of mechanical properties could play a role in stress transmission, although the impact seemed small when investigating the anisotropy of the plough pan (cf. Fig. 8). However, the matter of anisotropy requires further investigation and empirical evidence in order to validate any theoretical models.

It should be noted that patterns of stress decay with depth have been reported in the literature than could not be satisfactorily reproduced by Eqs. (1)–(3) (Trautner and Arvidsson, 2003; Richards and Peth, 2009; Lamandé and Schjøning, 2011a,b,c). Apart from the issues discussed above (i.e. inaccuracies in the stress readings, inappropriate upper stress boundary conditions), the reasons for these observations could be a very strong soil layering or a different mode of stress transmission such as preferential stress transmission (force chains) as observed in granular materials (see e.g. Keller et al., 2013; Nawaz et al., 2013). Differences in Young's modulus between soil layers (topsoil, plough pan, subsoil) could result from variations in soil texture, organic material, bulk density or soil matric potential of the individual layers. Unfortunately, very little is known about the Young's modulus (and the Poisson's ratio) of (different layers of) arable soils and how they are affected by soil texture, soil structure and soil moisture, despite a lot of data on compression curves reported in the literature. Measurements by Trautner and Arvidsson (2003) were performed on a clay soil (40–53% clay

content) mostly under dry to very dry conditions, and the observed differences between measurements and predictions of vertical soil stress using Eq. (3) were associated with the structure of the dry soil with ‘pillars’ separated by large vertical desiccation cracks. The soil profile presented by Richards and Peth (2009) included a 0.2 m thick plough pan and the pattern of stress decay reported was similar to that shown here in Fig. 6d. Wiermann et al. (2000) and Zink et al. (2010) found a larger stress attenuation in conservation tillage as compared with conventionally tilled soil. Zink et al. (2010) also measured significantly different tyre-soil contact areas in the two tillage systems. Lamandé and Schjønning (2011c) showed that there was a distinct difference in stress transmission between a regularly ploughed topsoil and the subsoil, with a more direct stress transmission (i.e. less stress attenuation) in the topsoil; when considering the subsoil only (0.3–0.9 m depth) ν was close to 3. Their results could be explained with the help of our simulations of a (weak) topsoil over a (stiffer) subsoil: a difference in stiffness between these layers increases the vertical stress (Fig. 9), although the simulated effect was smaller than measured by Lamandé and Schjønning (2011c). Furthermore, it is interesting to note that their measurements were made on a soil with a texture similar to the Vallø soil (Table 1), where we observed the largest negative bias at 0.3 m depth (Table 3).

Finally, this paper only deals with the vertical component of the soil stress. Most soil compaction research has focused on vertical stress, although the complete stress state is of relevance for changes in soil functions due to mechanical soil stresses induced by agricultural machinery (e.g. Horn, 2003; Berisso et al., 2013). For example, volume change (i.e. compaction) is a function of the mean normal stress (and not the vertical stress), and distortion is a result of the shear stress components (e.g. Koolen and Kuipers, 1983). We have a relatively good understanding of the transmission of vertical stress, but little knowledge regarding the magnitude and distribution of other stress components. A complete evaluation of models for stress transmission is only possible when considering the complete stress state. We suggest that further research on stress transmission in arable soil is needed.

5. Conclusions

This paper demonstrates that a comparison between the measured and simulated soil stress induced by agricultural machinery is not straightforward, because (i) measurements of stress in soil may be biased because transducers do not read true stresses (but the reliability of the stress transducers is normally not known), and (ii) the performance of simulations of soil stress is greatly affected by the magnitude and distribution of the applied stress (e.g. the tyre-soil contact stress), i.e. the upper stress boundary condition (which is typically unknown a priori).

For the five soils investigated here, we obtained an average “concentration factor” (ν) of 3.5 (for stress propagating from the 0.1 to 0.7 m depths). It is interesting that this was very close to $\nu = 3$, which corresponds to the classical Boussinesq (1885) solution. That is, the measured stress transmission followed the stress decay pattern obtained from linear elasticity theory for the conditions investigated in this paper. This was the case even though the soils investigated did not behave in a fully elastic manner.

Finite element simulations indicated that for an elasto-plastic layered soil the transmission of vertical stresses is not appreciably different from that in a homogeneous isotropic linear-elastic soil unless large differences in soil stiffness between the layers are considered.

We noted that estimates of ν were strongly dependent on the reliability of stress measurements, the accuracy of stress transducer depths, and the upper stress boundary condition used for

simulations. Furthermore, the data structure of the measurements (e.g. measurements of vertical stress in one dimension vs. measurements of vertical stress in three dimensions) affects the estimate of ν .

Our results highlight the importance of accurate stress readings and realistic surface stress boundary conditions. Future research on stress transmission should include the complete stress state. A more complete knowledge of the mechanical properties of arable soil and their directional dependence is needed in order to advance our quantitative understanding of stress transmission.

Acknowledgements

The measurements reported here were funded by the Swedish Farmers Foundation for Agricultural Research (SLF). The completion of this study was performed in the context of the ‘PredICTor’ (Preparing for the EU Soil Framework Directive by optimal use of Information and Communication Technology across Europe) project, which is funded by the Swiss Federal Office for Agriculture (BLW) and the Danish Ministry of Food, Agriculture and Fisheries via the European Commission’s ERA-NET “Coordination of European Research within ICT and Robotics in Agriculture and Related Environmental Issues” (ICT-AGRI) under the 7th Framework Programme for Research, and the “StressSoil” project funded by the Danish Research Council for Technology and Production Sciences (Project No.11-106471). The editorial assistance of Sally Selvadurai, Assist-Ed, Montréal is gratefully acknowledged. The two anonymous reviewers are thanked for valuable comments on the manuscript.

References

- Arvidsson, J., Andersson, S., 1997. Determination of soil displacement by measuring the pressure of a column of liquid. In: Proc. 14th Int. Conf. ISTRO, Puławy, PL, pp. 47–50.
- Arvidsson, J., Keller, T., 2007. Soil stress as affected by wheel load and tyre inflation pressure. *Soil Till. Res.* 96, 284–291.
- Arvidsson, J., Traunter, A., Keller, T., 2002. Influence of tyre inflation pressure on stress and displacement in the subsoil. *Adv. Geocol.* 35, 331–338.
- Berisso, F.E., Schjønning, P., Lamandé, M., Weisskopf, P., Stettler, M., Keller, T., 2013. Effects of the stress field induced by a running tyre on the soil pore system. *Soil Till. Res.* 131, 36–46.
- Berli, M., Accorsi, M.L., Or, D., 2006a. Size and shape evolution of pores in viscoplastic matrix under compression. *Int. J. Numer. Analyt. Methods Geomech.* 30, 1259–1281.
- Berli, M., Eggers, C.G., Accorsi, M.L., Or, D., 2006b. Theoretical analysis of fluid inclusion for in situ soil stress and deformation measurements. *Soil Sci. Soc. Am. J.* 70, 1441–1452.
- Berli, M., Kirby, J.M., Springman, S.M., Schulin, R., 2003. Modelling compaction of agricultural subsoils by tracked construction machinery under various moisture conditions. *Soil Till. Res.* 73, 57–66.
- Berli, M., Kulli, B., Attinger, W., Springman, S.M., Flüher, H., Schulin, R., 2004. Compaction of agricultural and forest subsoils by tracked heavy construction machinery. *Soil Till. Res.* 75, 37–52.
- Boizard, H., Won Yoon, S., Leonard, J., Lheureux, S., Cousin, I., Roger-Estrade, J., Richard, G., 2013. Using a morphological approach to evaluate the effect of traffic and weather conditions on the structure of a loamy soil in reduced tillage. *Soil Till. Res.* 127, 34–44.
- Boussinesq, J., 1885. *Application des Potentiels à l'étude de l'équilibre et du Mouvement des Solides Élastiques*. Gauthier-Villars, Paris, pp. 30.
- Davis, R.O., Selvadurai, A.P.S., 1996. *Elasticity and Geomechanics*. Cambridge University Press, Cambridge.
- Davis, R.O., Selvadurai, A.P.S., 2002. *Plasticity and Geomechanics*. Cambridge University Press, Cambridge.
- Défossez, P., Richard, G., Boizard, H., O'Sullivan, M.F., 2003. Modeling change in soil compaction due to agricultural traffic as function of soil water content. *Geoderma* 116, 89–105.
- Dexter, A.R., Horn, R., Holloway, R., Jakobsen, B.F., 1988. Pressure transmission beneath wheels in soils on the Eyre peninsula of South Australia. *J. Terramech.* 25, 135–147.
- Dörner, J., Horn, R., 2009. Direction-dependent behaviour of hydraulic and mechanical properties in structured soils under conventional and conservation tillage. *Soil Till. Res.* 102, 225–232.
- Fröhlich, O.K., 1934. *Druckverteilung im Baugrunde*. Springer Verlag, Wien, pp. 178.

- Horn, R., 1990. Structure effects on strength and stress distribution in arable soils. In: Proc. Int. Summer Meeting of ASAE, 24–27 June 1990, Columbus, Ohio, pp. 8–20.
- Horn, R., 2003. Stress–strain effects in structured unsaturated soils on coupled mechanical and hydraulic processes. *Geoderma* 116, 77–88.
- Johnson, C.E., Burt, E.C., 1990. A method of predicting soil stress state under tires. *Trans. Am. Soc. Agric. Eng.* 33, 713–717.
- Keller, T., Lamandé, M., Peth, S., Berli, M., Delenne, J.-Y., Baumgarten, W., Rabbel, W., Radjai, F., Rajchenbach, J., Selvadurai, A.P.S., Or, D., 2013. An interdisciplinary approach towards improved understanding of soil deformation during compaction. *Soil Till. Res.* 128, 61–80.
- Keller, T., 2005. A model for prediction of the contact area and the distribution of vertical stress below agricultural tyres from readily-available tyre parameters. *Biosyst. Eng.* 92, 85–96.
- Keller, T., Arvidsson, J., Schjønning, P., Lamandé, M., Stettler, M., Weisskopf, P., 2012. In situ subsoil stress–strain behavior in relation to soil precompression stress. *Soil Sci.* 177, 490–497.
- Keller, T., Arvidsson, J., 2004. Technical solutions to reduce the risk of subsoil compaction. *Soil Till. Res.* 79, 171–205.
- Keller, T., Arvidsson, J., 2007. Compressive properties of some Swedish and Danish structured agricultural soils measured in uniaxial compression tests. *Eur. J. Soil Sci.* 58, 1373–1381.
- Keller, T., Défossez, P., Weisskopf, P., Arvidsson, J., Richard, G., 2007. *SoilFlex: A model for prediction of soil stresses and soil compaction due to agricultural field traffic*. *Soil Till. Res.* 93, 391–411.
- Keller, T., Lamandé, M., 2010. Challenges in the development of analytical soil compaction models. *Soil Till. Res.* 111, 54–64.
- Kirby, J.M., 1999. Soil stress measurement: Part 1, transducer in a uniform stress field. *J. Agric. Eng. Res.* 72, 151–160.
- Koolen, A.J., Kuipers, H., 1983. *Agricultural Soil Mechanics*. Springer-Verlag, Berlin.
- Lamandé, M., Keller, T., Berisso, F.E., Stettler, M., Schjønning, P., 2014. Accuracy of soil stress measurements: Calibration of four transducers in the field. *Soil Till. Res.* (In revision).
- Lamandé, M., Schjønning, P., 2011a. Transmission of vertical stress in a real soil profile. Part I: Site description, evaluation of Söhne model, and the effect of topsoil tillage. *Soil Till. Res.* 114, 57–70.
- Lamandé, M., Schjønning, P., 2011b. Transmission of vertical stress in a real soil profile. Part II: Effect of tyre size, inflation pressure and wheel load. *Soil Till. Res.* 114, 71–77.
- Lamandé, M., Schjønning, P., 2011c. Transmission of vertical stress in a real soil profile. Part III: Effect of soil water content. *Soil Till. Res.* 114, 78–85.
- Lamandé, M., Schjønning, P., Tøgersen, F.A., 2007. Mechanical behaviour of an undisturbed soil subjected to loadings: effects of load and contact area. *Soil Till. Res.* 97, 91–106.
- Nawaz, M.F., Bourrié, G., Trolard, F., 2013. Soil compaction impact and modelling. A review. *Agron. Sust. Dev.* 33, 291–309.
- Pagliai, M., Marsili, A., Servadio, P., Vignozzi, N., Pellegrini, S., 2003. Changes in some physical properties of a clay soil in Central Italy following the passage of rubber tracked and wheeled tractors of medium power. *Soil Till. Res.* 73, 119–129.
- Peth, S., Horn, R., Fazekas, O., Richards, B.G., 2006. Heavy soil loading and its consequence for soil structure, strength, and deformation of arable soils. *J. Plant Nutr. Soil Sci.* 169, 775–783.
- Pytka, J., 2005. Effects of repeated rolling of agricultural tractors on soil stress and deformation state in sand and loess. *Soil Till. Res.* 82, 77–88.
- Poulos, H.G., Davis, E.H., 1974. *Elastic Solutions for Rock and Soil Mechanics*. Wiley, New York.
- Ram, R.B., 1984. Pressure measurement in the soil under the load. *Soil Till. Res.* 4, 137–145.
- Richards, B.G., Peth, S., 2009. Modelling soil physical behaviour with particular reference to soil science. *Soil Till. Res.* 102, 216–224.
- Selvadurai, A.P.S., 2000. *Partial Differential Equations in Mechanics, Vol.2. The Biharmonic Equation, Poisson's Equation*. Springer-Verlag, Berlin.
- Selvadurai, A.P.S., 2013. On Fröhlich's solution for Boussinesq's problem. *Int. J. Numer. Analyt. Methods Geomech.*, <http://dx.doi.org/10.1002/nag.2240>.
- Shames, I.H., Cozzarelli, F.A., 1997. *Elastic and Inelastic Stress Analysis*. Taylor & Francis, Washington DC.
- Söhne, W., 1953. Druckverteilung im Boden und Bodenverformung unter Schlep-
perreifen. *Grundlagen der Landtechnik* 5, 49–63.
- Trautner, A., Arvidsson, J., 2003. Subsoil compaction caused by machinery traffic on a Swedish Eutric Cambisol at different soil water contents. *Soil Till. Res.* 73, 107–118.
- von Mises, R., 1913. *Mechanik der festen Körper im plastisch-deformablen Zustand*. *Nachrichten von der Königlichen Gesellschaft der Wissenschaften zu Göttingen. Mathematisch-Physikalische Klasse* 1, 582–592.
- Weiler, W.A., Kulhawy, F.H., 1982. Factors affecting stress cell measurements in soil. *J. Geotechnical Eng. Division, Proc. Am. Soc. Civil Engineers* 108, 1529–1548.
- Wiermann, C., Werner, D., Horn, R., Rostek, J., Werner, B., 2000. Stress/strain processes in a structured unsaturated silty loam Luvisol under different tillage treatments in Germany. *Soil Till. Res.* 53, 117–128.
- Zink, A., Fleige, H., Horn, R., 2010. Load risks of subsoil compaction and depths of stress propagation in arable Luvisols. *Soil Sci. Soc. Am. J.* 74, 1733–1742.